

# LLMC+: Benchmarking Vision-Language Model Compression with a Plug-and-play Toolkit

Chengtao Lv<sup>1, 2\*</sup>, Bilang Zhang<sup>2, 3\*</sup>, Yang Yong<sup>2</sup>, Ruihao Gong<sup>2, 3†</sup>, Yushi Huang<sup>2, 4\*</sup>,  
Shiqiao Gu<sup>2</sup>, Jiajun Wu<sup>3</sup>, Yumeng Shi<sup>1</sup>, Jinyang Guo<sup>3</sup>, Wenyu Wang<sup>1†</sup>

<sup>1</sup>Nanyang Technological University, <sup>2</sup>SenseTime Research

<sup>3</sup>Beihang University, <sup>4</sup>Hong Kong University of Science and Technology

{chengtao001, yumeng001}@e.ntu.edu.sg, wangwy@ntu.edu.sg

{zhangbilang, yongyang, gongruihao, huangyushil, gushiqiao}@sensetime.com

## Abstract

Large Vision-Language Models (VLMs) exhibit impressive multi-modal capabilities but suffer from prohibitive computational and memory demands, due to their long visual token sequences and massive parameter sizes. To address these issues, recent works have proposed training-free compression methods. However, existing efforts often suffer from three major limitations: (1) Current approaches do not decompose techniques into comparable modules, hindering fair evaluation across spatial and temporal redundancy. (2) Evaluation confined to simple single-turn tasks, failing to reflect performance in realistic scenarios. (3) Isolated use of individual compression techniques, without exploring their joint potential. To overcome these gaps, we introduce LLMC+, a comprehensive VLM compression benchmark with a versatile, plug-and-play toolkit. LLMC+ supports over 20 algorithms across five representative VLM families and enables systematic study of token-level and model-level compression. Our benchmark reveals that: (1) Spatial and temporal redundancies demand distinct technical strategies. (2) Token reduction methods degrade significantly in multi-turn dialogue and detail-sensitive tasks. (3) Combining token and model compression achieves extreme compression with minimal performance loss. We believe LLMC+ will facilitate fair evaluation and inspire future research in efficient VLM. Our code is available at <https://github.com/ModelTC/LightCompress>.

## 1 Introduction

Recently, Large Language Models (LMMs) (Touvron et al. 2023; Liu et al. 2024a; Brown et al. 2020) have achieved rapid advancements in Natural Language Processing (NLP), which has become a significant milestone in the AI revolution. This breakthrough has quickly extended to vision modalities: mainstream Vision Language Models (VLMs) (Liu et al. 2023, 2024b; Wang et al. 2024a; Chen et al. 2024c) typically encode visual inputs into tokens and unify multiple modalities within a shared embedding space, demonstrating strong visual-language understanding and generation capabilities in various tasks (Singh et al. 2019; Antol et al. 2015; Hudson and Manning 2019).

\*Work done during internships at SenseTime Research.

†Corresponding authors.

Copyright © 2026, Association for the Advancement of Artificial Intelligence ([www.aaai.org](http://www.aaai.org)). All rights reserved.

However, their remarkable capabilities can be largely attributed to two aspects: 1) The number of visual tokens often reaches hundreds or even thousands, dominating the input. For example, images in LLaVA-NeXT (Liu et al. 2024c) are converted into 2,880 tokens. While in video streams or high-resolution scenarios, the number of tokens increases dramatically, further intensifying the computational costs. 2) VLMs have massive memory footprints (e.g., billion-scale parameters). Some large-scale VLMs, such as Qwen2.5-VL-72B (Wang et al. 2024a), consume approximately 140GB of memory for storage, becoming a major GPU memory bottleneck during inference. These two issues constrain their widespread application on resource-limited devices.

To effectively mitigate intractable computational and memory overhead, several training-free compression works have been proposed successively, which can be briefly classified into two fields: 1) *token-level compression*. These methods typically reduce less salient visual tokens through token reduction (Bolya et al. 2022; Chen et al. 2024b). 2) *model-level compression*. Their primary objective is to squeeze model weights through techniques like quantization (Gong et al. 2025b), network pruning (Sun et al. 2023), and low-rank factorization (Wang et al. 2024b).

Nevertheless, three worrisome problems still appear in current training-free compression research for VLMs. First, existing methods often target different types of redundancy (e.g., spatial or temporal) with distinct technical dimensions, leading to a lack of fair comparison and in-depth analysis across these dimensions. Second, these methods are limited to evaluation on general single-turn VQA tasks, lacking comprehensive assessments on challenging and practical tasks. Third, they typically rely on a single compression measure, without exploring the risks and potential of joint multiple compression strategies.

To this end, this paper presents LLMC+, a VLM compression benchmark with a versatile toolkit covering *token-level* and *model-level* compression. Specifically, LLMC+ supports over 20 compression algorithms and five different families of VLMs. 1) Based on LLMC+, we introduce a novel token reduction taxonomy specifically for handling spatial and temporal redundancy. We further distill their core technical dimensions, covering metrics (*attention-based* vs. *similarity-based*), solutions (*merge* vs. *prune*), and video

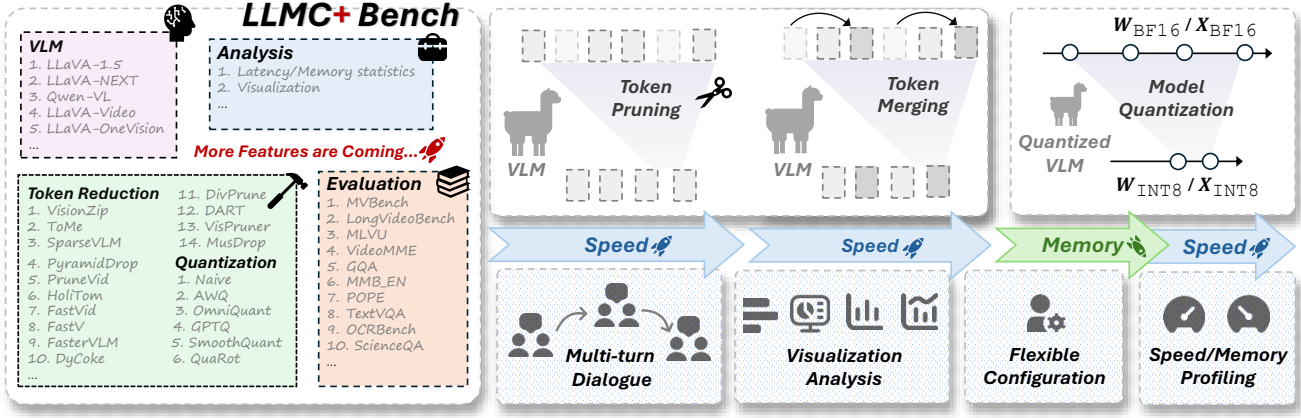


Figure 1: Illustration of our proposed powerful toolkit, LLMC+. Due to its high flexibility and versatility, we build a VLM compression benchmark upon it and conduct an in-depth analysis.

segmentation strategies (*fixed* vs. *dynamic*). Extensive experiments are conducted along these dimensions, accompanied by in-depth analysis. 2) Besides, we evaluate VLMs on practical task scenarios, such as multi-turn dialogue and detail-sensitive tasks like OCR and DocVQA, to uncover potential risks introduced by compression. 3) Finally, we combine token reduction and quantization to achieve extreme compression. We deploy quantized kernels on hardware to validate real acceleration and memory saving. Our benchmark reveals that 1) Spatial and temporal redundancy require distinct core strategies to be handled effectively. 2) Token reduction methods suffer from non-trivial performance degradation on practical tasks. 3) Combining multiple techniques enables extreme compression with accuracy guarantees.

We emphasize that the contributions of our LLMC+ can be summarized as follows:

- *Versatile Toolkit.* LLMC+ is the **first** plug-and-play compression toolkit specifically designed for VLMs, supporting over 20 compression algorithms across five different families of VLMs with flexible configuration.
- *Modular Comparison.* We construct a comprehensive taxonomy for token reduction that comprises all core technical modules, and conduct systematic evaluations for each module to ensure fair comparison.
- *Practical Evaluation.* Our findings highlight flaws in current evaluation practices and advocate for integrating our proposed practical evaluations into future evaluation standards.
- *Best Practice.* By following the modular guidelines proposed in this paper and combining token reduction with quantization, we achieve extreme compression.

## 2 LLMC+ Implementation

To enable comprehensive and fair comparison, we develop a versatile compression toolkit for VLMs. We highlight several key features in Fig. 1.

### 2.1 Various Algorithms and Models

LLMC+ supports a wide range of compression schemes, which can be broadly categorized into two fields. The first category includes 15 token reduction algorithms that concentrate on accelerating inference speed. The second category comprises model compression methods, covering 6 quantization algorithms, including both weight-only and weight-activation quantization. Moreover, LLMC+ integrates VLMs from different families, ranging from traditional image-based VLMs to video-oriented ones, including LLaVA-1.5 (Liu et al. 2023), LLaVA-NeXT (Liu et al. 2024c), Qwen2.5-VL (Bai et al. 2025), Video-LLaVA (Lin et al. 2023), and LLaVA-OneVision (Li et al. 2024a).

### 2.2 Flexible Configuration

The modular design of LLMC+ facilitates modality-aware compression (e.g., Vision Tower and LLM), seamless integration of diverse compression techniques (e.g., token reduction and quantization), multi-turn dialogues, and convenient configuration for latency/memory profiling and visualization. LLMC+ enables developers to perform customized analysis and compression tailored to their specific needs.

### 2.3 Benchmarks

LLMC+ is integrated with LMMs-Eval (Zhang et al. 2024a) for evaluation. For image tasks, we conduct experiments on nine widely used image understanding benchmarks, including visual question answering benchmarks such as GQA (Hudson and Manning 2019), ScienceQA (Saikh et al. 2022), TextVQA (Singh et al. 2019), and VizWiz (Bigham et al. 2010), as well as multi-modal reasoning benchmarks such as MMBench (Liu et al. 2024e), MME (Fu et al. 2023), POPE (Li et al. 2023b), OCRBench (Liu et al. 2024f), and DocVQA (Tito, Karatzas, and Valveny 2023). For video tasks, we select four standard video understanding benchmarks: MVbench (Li et al. 2024b), LongVideoBench (Wu et al. 2024), MLVU (Zhou et al. 2024), and VideoMME (Fu et al. 2025). These benchmarks cover complex scenarios and

Method	Venue	Vision		Language		Progressive
		Prune	Merge	Prune	Merge	
ToMe	ICLR 2023	X	S	X	X	✓
FastV	ECCV 2024	X	X	A	X	✗
SparseVLM	ICML 2025	X	X	A	S	✓
PDrop	CVPR 2025	X	X	A	X	✓
VisionZip	CVPR 2025	A	S	X	X	✗
VisPruner	ICCV 2025	A+S	X	X	X	✗
DART	EMNLP 2025	X	X	S	X	✗
DivPrune	CVPR 2025	S	X	X	X	✗
MustDrop	arXiv 2024	A	S	A	X	✗
HoliTom	NeurIPS 2025	X	S	X	S	✗

Table 1: Solutions for spatial redundancy. “A” and “S” denote attention- and similarity-based metrics, respectively.

Method	Venue	Segment	Prune	Merge
DyCoke	CVPR 2025	F	✓	✗
PruneVid	ACL 2025	D	✗	✓
FastVID	NeurIPS 2025	D	✗	✓
HoliTom	NeurIPS 2025	D	✗	✓

Table 2: Solutions for temporal redundancy. “F” and “D” denote Fixed and Dynamic segmentation strategies.

varying durations, enabling a comprehensive evaluation of effectiveness and generalization ability for these methods.

### 3 Dive into Token Reduction

In this section, we first present our taxonomy for addressing spatial and temporal redundancy (Sec. 3.1), which comprises two core technical aspects, respectively. For spatial redundancy, we conduct experiments in the vision (Sec. 3.2) and language components (Sec. 3.3) separately. For temporal redundancy, we distill a two-step pipeline and evaluate key techniques at each step (Sec. 3.4).

#### 3.1 Taxonomy

Token reduction primarily aims to eliminate redundancy in visual inputs. While images exhibit *spatial redundancy*, videos additionally contain *temporal redundancy*.

First, we present a taxonomy of methods designed to address spatial redundancy, as demonstrated in Tab. 1. Based on different perspectives, we divide them into the following categories:

- *Attention-based vs. Similarity-based metric.* Attention-based metrics typically rely on the question prompt or the [CLS] token, while similarity-based metrics measure the pairwise distance between tokens.
- *Prune vs. Merge.* Pruning discards insignificant visual tokens, whereas merging fuses them into other tokens.

Similarly, we categorize methods (see Tab. 2) addressing temporal redundancy into the following types:

- *Fixed vs. Dynamic segmentation.* Fixed segmentation partitions frames into segments of equal length, whereas dynamic segmentation generates segments that may vary in length.
- *Prune vs. Merge.* Similar to the above, but primarily applied to consecutive frames.

#### 3.2 Token Reduction in Vision Tower

We report the detailed results of token reduction schemes for Vision Tower in Tab. 3. It is worth noting that for each row, like “VisionZip PA” indicates the use of an Attention-based metric to Prune the unimportant tokens. We have several key observations: (1) *Prune-based methods generally outperform Merge-based ones in Vision Tower.* For example, three prune-based methods significantly outperform “ToMe MS” by a large margin. (2) *Similarity-based and Attention-based metrics, such as VisionZip PA (Yang et al. 2025b) and DivPrune PS (Alvar et al. 2025), exhibit only trivial differences in accuracy for most settings.* In detail, [CLS] attention serves as a strong indicator of token importance within the encoder and has demonstrated superior performance compared to other methods, as evidenced by its adoption in several previous works (Yang et al. 2025b; Zhang et al. 2024b; Liu et al. 2024d). However, for some advanced Vision Towers that cannot obtain [CLS] attention, such as SigLIP (Zhai et al. 2023). We believe there are two possible solutions. The first is to apply a similarity-based token pruning method, such as DivPrune PS (Alvar et al. 2025). The second is to reintegrate the SigLIP head into the model to generate [CLS] token, which incurs negligible computational overhead.

Besides, some methods apply token reduction in the shallow layers of Vision Tower. For instance, MustDrop MS (Liu et al. 2024d) performs spatial merge with sliding windows in the first layer of Vision Tower, while ToMe MS (Bolya et al. 2022) adopts a progressive token reduction strategy, where tokens are gradually pruned layer by layer during forward inference. To compare the impact of applying these methods at different depths, we measure their performance when applied to either shallow or deep layers of Vision Tower. Tab. 4 shows that applying token reduction to shallow layers leads to significant accuracy degradation, while offering slight improvements in prefill time. Therefore, *we recommend performing token reduction at the last layer of Vision Tower for a better trade-off between efficiency and accuracy.* However, these methods are not applicable to models like Qwen2.5-VL (Bai et al. 2025), because they occur before the model’s built-in spatial token merger module.

#### 3.3 Token Reduction in LLM

In contrast to text-agnostic token reduction methods applied within Vision Tower, token reduction within the LLM often leverages the question prompt as guidance for identifying important tokens. These methods typically perform token reduction in the shallow layers of the LLM. For a fair comparison, we implement all methods in our taxonomy (Tab. 1) at 5-th layer of the LLM during assessment. *The effectiveness of methods in LLM varies substantially across model families.* For instance, within the LLaVA family, prune-based approaches (i.e., FastV PA (Chen et al. 2024b), SparseVLM PA (Zhang et al. 2024c), and DART PS (Wen et al. 2025)) consistently outperform merge-based

<sup>1</sup>The seven benchmarks include GQA, MMB\\_EN, MME, POPE, TextVQA, VizWiz\\_VQA, and ScienceQA. Detailed results are provided in the **Appendix**.

Model	Method	Type	Acc.	Rel.	Acc.	Rel.	Acc.	Rel.
<i>Upper Bound, 576 Tokens (100%)</i>								
Vanilla		-	64.3	100%	64.3	100%	64.3	100%
<i>192 Tokens (↓ 66.7%)</i>								
LLaVA-1.5-7B (Liu et al. 2024b)	VisionZip (Yang et al. 2025b)	PA	62.9	97.9%	62.1	96.7%	60.5	94.1%
	VisPruner (Zhang et al. 2024b)	PS	62.5	97.2%	61.3	95.4%	59.7	92.8%
	DivPrune (Alvar et al. 2025)	PS	62.9	97.8%	62.4	97.1%	60.9	94.7%
	ToMe (Bolya et al. 2022)	MS	61.6	95.8%	61.0	94.9%	59.2	92.1%
	VisionZip (Yang et al. 2025b)	MS	60.8	94.5%	59.4	92.4%	56.3	87.5%
	MustDrop (Liu et al. 2024d)	MS	61.7	95.9%	59.3	92.3%	52.0	80.9%
	VisionZip (Yang et al. 2025b)	PA+MS	62.9	97.9%	62.2	96.7%	60.4	93.9%
<i>Upper Bound, ~2880 Tokens (100%)</i>								
Vanilla		-	68.6	100%	68.6	100%	68.6	100%
LLaVA-NeXT-7B (Liu et al. 2024c)	VisionZip (Yang et al. 2025b)	PA	66.8	97.3%	64.9	94.6%	62.2	90.6%
	VisPruner (Zhang et al. 2024b)	PS	64.9	94.6%	62.7	91.4%	59.6	86.8%
	DivPrune (Alvar et al. 2025)	PS	65.6	95.5%	63.8	93.0%	62.3	90.8%
	VisionZip (Yang et al. 2025b)	MS	62.7	91.4%	60.1	87.6%	56.1	81.8%
	MustDrop (Liu et al. 2024d)	MS	64.9	94.5%	61.3	89.2%	-	-
<i>Upper Bound, 1000 Tokens</i>								
Vanilla		-	79.3	100%	79.3	100%	79.3	100%
Qwen2.5-VL-7B (Bai et al. 2025)	VisionZip (Yang et al. 2025b)	PA	77.9	98.2%	75.9	95.7%	70.7	89.2%
	VisPruner (Zhang et al. 2024b)	PS	76.8	96.8%	74.4	93.9%	68.8	86.7%
	DivPrune (Alvar et al. 2025)	PS	77.3	97.4%	75.6	95.3%	71.5	90.2%
	VisionZip (Yang et al. 2025b)	MS	76.9	97.0%	74.6	94.1%	68.3	86.1%

Table 3: Average performance of different token reduction methods in Vision Tower across seven benchmarks<sup>1</sup>.

Method	Type	Acc.	Rel.	Prefill
<i>Upper Bound, 576 Tokens (100%)</i>				
LLaVA-1.5-7B (Liu et al. 2024b)	-	64.3	100%	27.3 ms
<i>Retain 192 Tokens in Average (↓ 66.7%)</i>				
ToMe <sup>*</sup> (Bolya et al. 2022)	MS	53.5	83.2%	16.6 ms
ToMe <sup>†</sup> (Bolya et al. 2022)	MS	62.4	97.0%	16.6 ms
MustDrop <sup>*</sup> (Liu et al. 2024d)	MS	58.8	91.4%	16.6 ms
MustDrop <sup>†</sup> (Liu et al. 2024d)	MS	61.7	95.9%	16.6 ms
<i>Retain 128 Tokens in Average (↓ 77.8%)</i>				
ToMe <sup>*</sup> (Bolya et al. 2022)	MS	45.3	70.5%	15.8 ms
ToMe <sup>†</sup> (Bolya et al. 2022)	MS	60.3	93.8%	16.0 ms
MustDrop <sup>*</sup> (Liu et al. 2024d)	MS	54.2	84.3%	16.0 ms
MustDrop <sup>†</sup> (Liu et al. 2024d)	MS	59.3	92.3%	16.2 ms

Table 4: Results of token reduction at different layers in Vision Tower. <sup>\*</sup> and <sup>†</sup> denote merging in the first and last layer.

schemes (e.g., HoliTom MS (Shao et al. 2025)). In contrast, for Qwen2.5-VL, HoliTom MS (Shao et al. 2025) demonstrates competitive performance. Token reduction methods applied within the LLM typically introduce additional computational overhead but tend to achieve better performance compared to those applied in Vision Tower. For instance, DART PS (Wen et al. 2025) can maintain nearly lossless performance on LLaVA-1.5-7B even when preserving only one-third of the visual tokens. *This also highlights a key limitation of attention-based metrics within the LLM.* They tend to assign higher attention scores to visual tokens that are spatially closer to text tokens (Zhang et al. 2024b) (See in the Appendix). Therefore, it is necessary to reconsider the use of attention-based metrics for token reduction in LLM.

After comparing prune and merge algorithms in both the vision and language components, we further investigate whether combining token prune and merge can lead to improved performance. Recent works (Yang et al. 2025b;

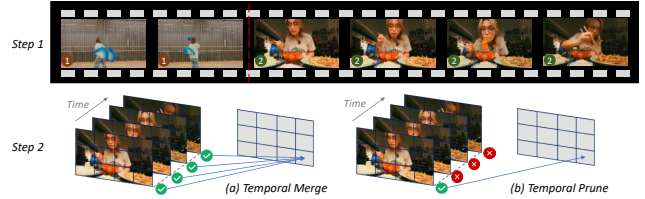


Figure 2: The pipeline of removing temporary redundancy in the two steps.

Zhang et al. 2024c) usually follow a two-step pipeline to integrate prune and merge: important tokens are first preserved through pruning, and then the remaining less informative contextual tokens are merged. Therefore, we select a representative algorithm from each of the vision and language parts for our experiments. As shown in Tab. 3 and Tab. 5, the standalone prune method and the combination (*i.e.*, PA+MS) are compared. It can be observed that in most cases, introducing merge in addition to pruning does not significantly improve the model’s performance, and in some settings, it even leads to slightly lower accuracy compared to prune alone.

### 3.4 From Image to Video

Although several token reduction methods for spatial redundancy have been discussed in the aforementioned sections, directly applying these solutions to video tasks overlooks a key characteristic of video data that necessitates a rethinking of traditional pruning strategies. Compared with images, videos naturally introduce an additional form of considerable redundancy: temporal redundancy. This redundancy primarily arises from similar tokens in adjacent frames, which fail to provide additional informative content. There-

Model	Method	Type	Acc.	Rel.	Acc.	Rel.	Acc.	Rel.
<i>Upper Bound, 576 Tokens (100%)</i>								
	Vanilla	-	64.3	100%	64.3	100%	64.3	100%
<i>192 Tokens (↓ 66.7%)</i>								
LLaVA-1.5-7B (Liu et al. 2024b)	FastV (Chen et al. 2024b)	PA	62.4	97.1%	60.9	94.7%	56.8	88.3%
	SparseVLM (Zhang et al. 2024c)	PA	63.3	98.5%	62.4	97.1%	60.0	93.3%
	DART (Wen et al. 2025)	PS	63.7	99.0%	62.9	97.9%	61.4	95.5%
	HoliTom (Shao et al. 2025)	MS	61.5	95.6%	60.1	93.5%	57.5	89.4%
<i>64 Tokens (↓ 88.9%)</i>								
<i>Upper Bound, ~2880 Tokens (100%)</i>								
	Vanilla	-	68.6	100%	68.6	100%	68.6	100%
<i>~640 Tokens (↓ 66.7%)</i>								
LLaVA-NeXT-7B (Liu et al. 2024c)	FastV (Chen et al. 2024b)	PA	65.8	95.9%	61.7	89.9%	56.0	81.5%
	SparseVLM (Zhang et al. 2024c)	PA	66.9	97.5%	64.8	94.5%	61.3	89.2%
	DART (Wen et al. 2025)	PS	67.2	98.0%	65.2	95.0%	62.1	90.5%
	HoliTom (Shao et al. 2025)	MS	64.7	94.2%	61.5	89.6%	54.6	79.6%
<i>Upper Bound, 1000 Tokens</i>								
	Vanilla	-	79.3	100%	79.3	100%	79.3	100%
<i>33.3% Tokens (↓ 66.7%)</i>								
Qwen2.5-VL-7B (Bai et al. 2025)	FastV (Chen et al. 2024b)	PA	75.9	95.7%	72.5	91.4%	64.5	81.3%
	SparseVLM (Zhang et al. 2024c)	PA	77.6	97.9%	76.1	95.9%	72.0	90.7%
	DART (Wen et al. 2025)	PS	76.6	96.6%	74.6	94.1%	69.2	87.3%
	HoliTom (Shao et al. 2025)	MS	77.2	97.4%	75.0	94.6%	69.8	88.1%

Table 5: Average performance of different token reduction methods in LLM across seven benchmarks.

Method	MR	RR	Segment	Prefill	MVBench	LongVideoBench	MLVU	VideoMME	Score	%
Duration					16 sec	1~60 min	3~120 min	1~60 min		
Vanilla	-	100%	-	290.7ms	58.35	56.55	63.10	58.51	59.13	100.0%
Fixed	50%	56.2%	0 ms	164.7 ms	58.67	55.87	63.65	59.22	59.35	100.4%
PruneVid	50%	54.6%	3.3 ms	159.5 ms	58.45	55.80	62.76	58.70	58.93	99.7%
FastVID	50%	56.2%	2.5 ms	165.7 ms	58.35	54.90	62.98	59.00	58.81	99.5%
Fixed	80%	30.3%	0 ms	88.1 ms	57.98	54.37	60.79	58.18	57.83	97.8%
PruneVid	80%	27.7%	3.3 ms	82.5 ms	57.80	54.53	61.89	57.34	57.89	97.9%
FastVID	80%	30.3%	2.5 ms	88.1 ms	57.90	54.82	61.69	57.81	58.06	98.2%
HoliTom	-	52.4%	35.5 ms	149.0 ms	57.70	56.17	63.42	59.33	59.16	100.1%
HoliTom	-	68.9%	35.5 ms	199.6 ms	58.35	55.80	63.30	58.85	59.08	99.9%

Table 6: Comparison of four video segmentation methods on LLaVA-OneVision (Li et al. 2024a). **Merge Rate** (MR) denotes the intra-segment merge ratio, whereas **Retention Rate** (RR) measures the overall token retention for an input. This also implies that even with the same Merge Rate, different segment lengths will lead to varying Retention Rates.

fore, recent studies (Tao et al. 2025; Fu et al. 2024; Shao et al. 2025; Huang, Zhou, and Han 2024; Shen et al. 2025) aim to reduce such redundancy.

Specifically, these approaches tailored for videos mainly follow a two-step paradigm (Fig. 2). In the first step, these algorithms partition a video into temporally ordered segments with high similarity, which often correspond to the same scene. In the second step, they reduce unimportant visual tokens within each segment while preserving informative ones. The remainder of this section explores how to perform these two steps to effectively reduce temporal redundancy.

**First step:** To thoroughly explore different segment partition strategies, we summarize four representative methods, covering DyCoke (Tao et al. 2025), FastVID (Shen et al. 2025), PruneVid (Huang, Zhou, and Han 2024), and HoliTom (Shao et al. 2025). To ensure a fair comparison, we apply a uniform merge strategy to highly similar tokens within each segment after partitioning. In addition to reporting performance under comparable compression ratios, we also provide the segmentation time and overall prefill time.

In Tab. 6, we report the detailed results of these schemes.

When the merge rate is relatively low (around 50%), all methods achieve near-lossless performance, demonstrating the substantial temporal redundancy inherent in video tasks. As more tokens are merged, the fixed segmentation strategy exhibits a noticeable drop in accuracy. In contrast, dynamic segmentation methods such as PruneVid (Huang, Zhou, and Han 2024) and FastVID (Shen et al. 2025) achieve better performance while retaining the same or even fewer tokens. In terms of segmentation latency, HoliTom incurs an additional overhead of 35.5ms largely due to its use of dynamic programming to determine segment boundaries, which introduces an  $\mathcal{O}(n^2)$  computational cost. In contrast, other dynamic segmentation methods (e.g., PruneVid, FastVID), require only 3.5ms and 2.5ms, making their latency negligible.

**Second step:** After obtaining high-quality segments, a natural question arises: *How can we eliminate the temporal redundancy of consecutive frames within each segment?* DyCoke (Tao et al. 2025) preserves the visual tokens in the first frame while pruning those in subsequent frames (Fig. 2 (b)), whereas PruneVid (Huang, Zhou, and Han 2024) merges similar tokens to reduce redundancy (Fig. 2 (a)). To com-

Method	MVBench	LongVideoBench	MLVU	VideoMME	Avg.
Duration	16 sec	1~60 min	3~120 min	1~60 min	
DyCoke*	58.35	63.10	63.58	59.44	61.12
DyCoke†	58.23	63.10	62.99	58.74	60.77
PruneVid*	57.28	63.30	63.30	59.55	60.86
PruneVid†	56.58	63.31	63.31	59.40	60.65

Table 7: Comparison between Temporal Merge (superscript \*) and Temporal Prune (superscript †).

Method	~640 Tokens		~320 Tokens		~160 Tokens	
	DOC	OCR	DOC	OCR	DOC	OCR
Vanilla	68.5	52.1	68.5	52.1	68.5	52.1
FastV	46.6	38.9	29.7	24.8	17.8	15.4
DART	54.6	44.2	42.3	35.4	29.4	26.8
SparseVLM	49.1	40.6	31.1	29.0	17.3	18.6
VisionZip	56.9	48.5	42.5	39.5	28.8	29.5
VisPruner	53.9	44.8	39.6	37.3	27.4	31.7
DivPrune	44.8	37.6	32.8	33.0	26.1	26.6

Table 8: DocVQA (Tito, Karatzas, and Valveny 2023) and OCRBench (Liu et al. 2024f) results of token reduction.

pare these two schemes, we conduct both temporal merge and prune experiments for DyCoke and PruneVid.

Interestingly, we observe similar results for these two algorithms (Tab. 7). Temporal merge outperforms temporal prune (61.22 vs. 60.77 for DyCoke and 60.86 vs. 60.65 for PruneVid). *These findings indicate that merge may be more suitable than prune for overcoming temporal redundancy.* The main reason is the high similarity between tokens at corresponding positions across consecutive frames within the same segment. See the Appendix for details.

### Finding 1.

**Spatial Redundancy:** ① Vision Tower: Similarity-based and Attention-based metrics perform comparably, while Prune generally outperforms Merge. ② LLM: Sophisticated metrics and solutions should be chosen to suit different scenarios.

**Temporal Redundancy:** Dynamic segmentation outperforms Fixed ones. Merge is slightly more effective than prune.

## 4 Compression Struggles in Practical Tasks

Although the aforementioned methods (Yang et al. 2025b; Zhang et al. 2024c; Wen et al. 2025; Alvar et al. 2025) have demonstrated strong performance on general single-turn VQA tasks, they neglect systematic evaluation on practical tasks. First, real-world applications often involve fine-grained tasks that require a far more precise understanding of visual details, such as DocVQA (Tito, Karatzas, and Valveny 2023) and OCRBench (Liu et al. 2024f). Second, modern inference engines (Zheng et al. 2024; Gong et al. 2025a) for VLMs widely use prefix caching in multi-turn dialogue, reusing encoded visual-text prefixes to reduce redundant computation. Hence, evaluating the effectiveness of compression techniques on both task types is essential.

Method	Text Info	Score
VisionZip (Yang et al. 2025b)	None	0.938
DivPrune (Alvar et al. 2025)	None	0.929
DART (Wen et al. 2025)	Low	0.903
FastV (Chen et al. 2024b)	High	0.896
SparseVLM (Zhang et al. 2024c)	High	0.882

Table 9: Performance comparison of various methods on multi-turn dialogue tasks.

**Fine-Grained Tasks.** We select two detail-sensitive tasks, DocVQA (Tito, Karatzas, and Valveny 2023) and OCRBench (Liu et al. 2024f), to evaluate the accuracy degradation introduced by token reduction under different compression ratios on LLaVA-NeXT-7B (Liu et al. 2024c). *In Tab. 8, we observe that the accuracy of token reduction on these tasks is still far from satisfactory.* For example, retaining approximately 160 tokens leads to non-trivial performance degradation on these tasks, with accuracy dropping to around 50%, in stark contrast to the around 80% accuracy achieved on general VQA benchmarks (Tab. 3 and Tab. 5). Therefore, subsequent works should place greater emphasis on these more challenging fine-grained tasks.

**Multi-Turn Tasks.** We further build a multi-turn dialogue dataset tailored for token reduction in a simple-yet-effective manner. Instead of constructing a dataset from scratch, we build upon the existing visual question answering benchmark, GQA (Hudson and Manning 2019), by selecting two semantically distinct questions for each image, serving as the first-turn and second-turn questions. Since the first-turn and second-turn questions are different, and their difficulty levels may vary randomly, we further swap the order of the two questions to create a new question pair. As a result, each question appears once in the first turn and once in the second turn, allowing us to eliminate randomness.

Moreover, rather than relying solely on traditional accuracy-based metrics, we focus on evaluating an algorithm’s consistency in multi-turn dialogue. Specifically, we are interested in the probability that a question is answered correctly in the second turn, if it can be answered correctly in the first turn. To compute this, we propose a novel metric that measures this conditional accuracy:

$$P(Q_2^T | Q_1^T) = \frac{P(Q_2^T, Q_1^T)}{P(Q_1^T)} \approx \frac{N(Q_2^T, Q_1^T)}{N(Q_1^T)} \quad (1)$$

where  $Q_i^T$  indicates that the question at turn  $i$  is answered correctly.  $P$  and  $N$  denote the probability and corresponding number. We select several representative algorithms and categorize them based on the extent to which they utilize textual information. As we can see in Tab. 9, text-agnostic schemes, such as VisionZip and DivPrune, surpass text-relevant ones (*i.e.*, FastV and SparseVLM). *This suggests that question-dependent approaches may prune visual tokens that are required in subsequent turns, leading to performance degradation in multi-turn dialogue scenarios.* Visualization results can be found in the Appendix.

Method	GQA	MMB_EN	MME	POPE	TextVQA	Avg (%)
LLaVA-1.5-7B	61.2	62.9	1805	85.5	48.6	100.0
FastV	56.1	61.8	1744	79.5	42.8	93.4
GPTQ	60.9	62.8	1790	85.1	48.3	99.5
GPTQ + FastV	55.3	60.5	1732	79.2	42.6	92.5
SQ	61.2	63.7	1781	85.4	48.5	99.9
SQ + FastV	56.0	61.2	1702	79.6	42.9	92.9
LLaVA-1.5-13B	62.6	68.3	1854	85.7	52.8	100.0
FastV	58.6	66.8	1747	80.7	45.1	93.0
GPTQ	62.2	67.4	1840	85.8	52.6	99.4
GPTQ + FastV	58.5	65.6	1749	80.8	44.9	92.6
SQ	62.6	68.5	1840	85.6	53.0	100.0
SQ + FastV	58.3	66.1	1757	80.6	44.9	92.8

Table 10: Results of joint token reduction and quantization on LLaVA-1.5, where SQ denotes SmoothQuant and 192 visual tokens are preserved for FastV.

**Finding 2.** Token reduction suffers from significant accuracy drops on fine-grained tasks, and prompt-dependent methods yield unsatisfactory results in multi-turn dialogue. Future work should give more attention to the performance in these tasks.

## 5 Achieving Extreme Compression

Although token reduction can significantly reduce inference latency, it does not lower the peak memory usage during inference. The rationale lies in the fact that model weights dominate memory consumption, which often accounts for over 90%, while token reduction primarily reduces the storage cost of the KV Cache (shown in Fig. 3). To further address the memory bottleneck in VLM inference, we adopt post-training quantization (Xiao et al. 2023; Frantar et al. 2022; Lin et al. 2024), which is more practical during deployment and application.

Following the categorization of quantization methods, we choose GPTQ (Frantar et al. 2022) as a representative algorithm for weight-only quantization (W4A16), and SmoothQuant (Xiao et al. 2023) for weight-activation quantization (W8A8). In Tab. 10, we present detailed results for the joint application of token reduction and quantization. We summarize the following key observations: 1) Using quantization alone (e.g., W8A8 and W4A16) can retain near-lossless accuracy on VLMs. When combined with token reduction, overall performance mainly depends on the effectiveness of the token reduction method. 2) W8A8 consistently achieves better accuracy than W4A16, regardless of whether token reduction is applied.

To further validate the actual speedup and memory savings of quantized VLM, we deploy LLaVA-NeXT-7B on an NVIDIA RTX 4090 GPU. We utilize the int8 kernel from vLLM (Kwon et al. 2023) for “LLM Backbone” and the int8 kernel from q8 (q8 team 2026) for “Vision Tower”. When the number of visual tokens decreases from 2487 to 1243 (50% is considered a safe pruning ratio (Chen et al. 2024b)), the model achieves a 1.56 $\times$  speedup, but with negligible change in memory usage. However, when combined with quantization, the model achieves a 2.54 $\times$  speedup along with a 1.64 $\times$  reduction in memory consumption. Therefore,

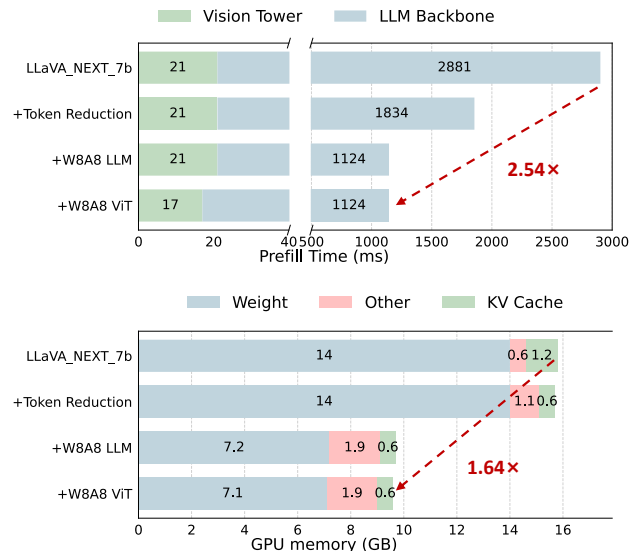


Figure 3: Real inference efficiency on LLaVA-NeXT (Liu et al. 2024c).

our recommended best practice is to combine token reduction with efficient *model-level* compression techniques, such as quantization.

**Finding 3.** Introducing relatively stable W8A8 or W4A16 quantization into token reduction yields greater compression rates without a significant performance drop.

## 6 Conclusion

In this study, we present a VLM compression benchmark with a versatile toolkit, dubbed LLMC+. We identify three major limitations in existing research and conduct comprehensive experiments to evaluate various compression methods. Our benchmark contributes in three key areas: (1) We explore diverse technical strategies for handling spatial and temporal redundancy. For each, we distill the core techniques and perform modular comparisons across related methods, and provide in-depth analysis. (2) Our benchmark systematically evaluates compression performance on fine-grained tasks and multi-turn dialogue, revealing the limitations of existing methods in practical scenarios. (3) We investigate the effectiveness and trade-offs of combining multiple compression methods (*i.e.*, token reduction and quantization). We expect our work to provide valuable insights and serve as a practical guide for the community in advancing more effective VLM compression techniques.

## 7 Acknowledgements

This work was supported by the Beijing Natural Science Foundation (QY24138), the Fundamental Research Funds for the Central Universities, the Postdoctoral Fellowship Program and China Postdoctoral Science Foundation (No. BX20250487).

## References

Alayrac, J.-B.; Donahue, J.; Luc, P.; Miech, A.; Barr, I.; Hasson, Y.; Lenc, K.; Mensch, A.; Millican, K.; Reynolds, M.; et al. 2022. Flamingo: a visual language model for few-shot learning. *Advances in neural information processing systems*, 35: 23716–23736.

Alvar, S. R.; Singh, G.; Akbari, M.; and Zhang, Y. 2025. Diproprune: Diversity-based visual token pruning for large multimodal models. In *Proceedings of the Computer Vision and Pattern Recognition Conference*, 9392–9401.

Antol, S.; Agrawal, A.; Lu, J.; Mitchell, M.; Batra, D.; Zitnick, C. L.; and Parikh, D. 2015. Vqa: Visual question answering. In *Proceedings of the IEEE international conference on computer vision*, 2425–2433.

Arif, K. H. I.; Yoon, J.; Nikolopoulos, D. S.; Vandierendonck, H.; John, D.; and Ji, B. 2025. HiRED: Attention-Guided Token Dropping for Efficient Inference of High-Resolution Vision-Language Models. In *Proceedings of the AAAI Conference on Artificial Intelligence*, volume 39, 1773–1781.

Bai, S.; Chen, K.; Liu, X.; Wang, J.; Ge, W.; Song, S.; Dang, K.; Wang, P.; Wang, S.; Tang, J.; et al. 2025. Qwen2. 5-vl technical report. *arXiv preprint arXiv:2502.13923*.

Bigham, J. P.; Jayant, C.; Ji, H.; Little, G.; Miller, A.; Miller, R. C.; Miller, R.; Tatarowicz, A.; White, B.; White, S.; et al. 2010. Vizwiz: nearly real-time answers to visual questions. In *Proceedings of the 23rd annual ACM symposium on User interface software and technology*, 333–342.

Bolya, D.; Fu, C.-Y.; Dai, X.; Zhang, P.; Feichtenhofer, C.; and Hoffman, J. 2022. Token merging: Your vit but faster. *arXiv preprint arXiv:2210.09461*.

Brown, T.; Mann, B.; Ryder, N.; Subbiah, M.; Kaplan, J. D.; Dhariwal, P.; Neelakantan, A.; Shyam, P.; Sastry, G.; Askell, A.; et al. 2020. Language models are few-shot learners. *Advances in neural information processing systems*, 33: 1877–1901.

Chen, H.; Lv, C.; Ding, L.; Qin, H.; Zhou, X.; Ding, Y.; Liu, X.; Zhang, M.; Guo, J.; Liu, X.; et al. 2024a. Db-llm: Accurate dual-binarization for efficient llms. *arXiv preprint arXiv:2402.11960*.

Chen, L.; Zhao, H.; Liu, T.; Bai, S.; Lin, J.; Zhou, C.; and Chang, B. 2024b. An image is worth 1/2 tokens after layer 2: Plug-and-play inference acceleration for large vision-language models. In *European Conference on Computer Vision*, 19–35. Springer.

Chen, Z.; Wu, J.; Wang, W.; Su, W.; Chen, G.; Xing, S.; Zhong, M.; Zhang, Q.; Zhu, X.; Lu, L.; et al. 2024c. Internvl: Scaling up vision foundation models and aligning for generic visual-linguistic tasks. In *Proceedings of the IEEE/CVF conference on computer vision and pattern recognition*, 24185–24198.

Dhouib, M.; Buscaldi, D.; Vanier, S.; and Shabou, A. 2025. Pact: Pruning and clustering-based token reduction for faster visual language models. In *Proceedings of the Computer Vision and Pattern Recognition Conference*, 14582–14592.

Frantar, E.; and Alistarh, D. 2023. Sparsegpt: Massive language models can be accurately pruned in one-shot. In *International conference on machine learning*, 10323–10337. PMLR.

Frantar, E.; Ashkboos, S.; Hoefer, T.; and Alistarh, D. 2022. Gptq: Accurate post-training quantization for generative pre-trained transformers. *arXiv preprint arXiv:2210.17323*.

Fu, C.; Chen, P.; Shen, Y.; Qin, Y.; Zhang, M.; Lin, X.; Yang, J.; Zheng, X.; Li, K.; Sun, X.; Wu, Y.; and Ji, R. 2023. MME: A Comprehensive Evaluation Benchmark for Multimodal Large Language Models. *arXiv preprint arXiv:2306.13394*.

Fu, C.; Dai, Y.; Luo, Y.; Li, L.; Ren, S.; Zhang, R.; Wang, Z.; Zhou, C.; Shen, Y.; Zhang, M.; et al. 2025. Videomme: The first-ever comprehensive evaluation benchmark of multi-modal llms in video analysis. In *Proceedings of the Computer Vision and Pattern Recognition Conference*, 24108–24118.

Fu, T.; Liu, T.; Han, Q.; Dai, G.; Yan, S.; Yang, H.; Ning, X.; and Wang, Y. 2024. Framefusion: Combining similarity and importance for video token reduction on large visual language models. *arXiv preprint arXiv:2501.01986*.

Gong, R.; Bai, S.; Wu, S.; Fan, Y.; Wang, Z.; Li, X.; Yang, H.; and Liu, X. 2025a. Past-future scheduler for llm serving under sla guarantees. In *Proceedings of the 30th ACM International Conference on Architectural Support for Programming Languages and Operating Systems, Volume 2*, 798–813.

Gong, R.; Ding, Y.; Wang, Z.; Lv, C.; Zheng, X.; Du, J.; Yong, Y.; Gu, S.; Qin, H.; Guo, J.; et al. 2025b. A survey of low-bit large language models: Basics, systems, and algorithms. *Neural Networks*, 107856.

Gou, J.; Yu, B.; Maybank, S. J.; and Tao, D. 2021. Knowledge distillation: A survey. *International journal of computer vision*, 129(6): 1789–1819.

Guo, J.; Liu, J.; and Xu, D. 2021. JointPruning: Pruning networks along multiple dimensions for efficient point cloud processing. *IEEE Transactions on Circuits and Systems for Video Technology*.

Guo, J.; Ouyang, W.; and Xu, D. 2020. Multi-Dimensional Pruning: A Unified Framework for Model Compression. In *CVPR*.

Guo, J.; Xu, D.; and Ouyang, W. 2023. Multidimensional Pruning and Its Extension: A Unified Framework for Model Compression. *IEEE Transactions on Neural Networks and Learning Systems*.

Guo, J.; Zhang, W.; Ouyang, W.; and Xu, D. 2020. Model compression using progressive channel pruning. *IEEE Transactions on Circuits and Systems for Video Technology*.

Han, J.; Du, L.; Wu, Y.; Zhou, X.; Du, H.; and Zheng, W. 2025. Adafv: Accelerating vlms with self-adaptive cross-modality attention mixture. *arXiv e-prints*, arXiv–2501.

Han, Y.; Liu, X.; Zhang, Z.; Ding, P.; Wang, D.; Chen, H.; Yan, Q.; and Huang, S. 2024. Filter, correlate, compress: Training-free token reduction for mllm acceleration. *arXiv preprint arXiv:2411.17686*.

He, C.; Ding, Y.; Guo, J.; Gong, R.; Qin, H.; and Liu, X. 2025. DA-KD: Difficulty-Aware Knowledge Distillation for Efficient Large Language Models. In *Forty-first International Conference on Machine Learning*.

Huang, X.; Zhou, H.; and Han, K. 2024. Prunevid: Visual token pruning for efficient video large language models. *arXiv preprint arXiv:2412.16117*.

Huang, Y.; Gong, R.; Liu, J.; Chen, T.; and Liu, X. 2024. TFMQ-DM: Temporal Feature Maintenance Quantization for Diffusion Models. *arXiv:2311.16503*.

Huang, Y.; Gong, R.; Liu, J.; Ding, Y.; Lv, C.; Qin, H.; and Zhang, J. 2025a. QVGen: Pushing the Limit of Quantized Video Generative Models. *arXiv:2505.11497*.

Huang, Y.; Gong, R.; Liu, X.; Liu, J.; Li, Y.; Lu, J.; and Tao, D. 2025b. Temporal Feature Matters: A Framework for Diffusion Model Quantization. *arXiv:2407.19547*.

Huang, Y.; Wang, Z.; Gong, R.; Liu, J.; Zhang, X.; Guo, J.; Liu, X.; and Zhang, J. 2025c. HarmoniCa: Harmonizing Training and Inference for Better Feature Caching in Diffusion Transformer Acceleration. *arXiv:2410.01723*.

Hudson, D. A.; and Manning, C. D. 2019. Gqa: A new dataset for real-world visual reasoning and compositional question answering. In *Proceedings of the IEEE/CVF conference on computer vision and pattern recognition*, 6700–6709.

J. Guo, W. Ouyang, and D. Xu. 2020. Channel pruning guided by classification loss and feature importance. In *AAAI*.

Kwon, W.; Li, Z.; Zhuang, S.; Sheng, Y.; Zheng, L.; Yu, C. H.; Gonzalez, J. E.; Zhang, H.; and Stoica, I. 2023. Efficient Memory Management for Large Language Model Serving with PagedAttention. In *Proceedings of the ACM SIGOPS 29th Symposium on Operating Systems Principles*.

Lan, X.; Yuan, Y.; Jie, Z.; and Ma, L. 2024. Vidcompress: Memory-enhanced temporal compression for video understanding in large language models. *arXiv preprint arXiv:2410.11417*.

Li, B.; Zhang, Y.; Guo, D.; Zhang, R.; Li, F.; Zhang, H.; Zhang, K.; Zhang, P.; Li, Y.; Liu, Z.; et al. 2024a. Llava-onevision: Easy visual task transfer. *arXiv preprint arXiv:2408.03326*.

Li, J.; Li, D.; Savarese, S.; and Hoi, S. 2023a. Blip-2: Bootstrapping language-image pre-training with frozen image encoders and large language models. In *International conference on machine learning*, 19730–19742. PMLR.

Li, K.; Wang, Y.; He, Y.; Li, Y.; Wang, Y.; Liu, Y.; Wang, Z.; Xu, J.; Chen, G.; Luo, P.; et al. 2024b. Mvbench: A comprehensive multi-modal video understanding benchmark. In *Proceedings of the IEEE/CVF Conference on Computer Vision and Pattern Recognition*, 22195–22206.

Li, Y.; Du, Y.; Zhou, K.; Wang, J.; Zhao, W. X.; and Wen, J.-R. 2023b. Evaluating object hallucination in large vision-language models. *arXiv preprint arXiv:2305.10355*.

Lin, B.; Ye, Y.; Zhu, B.; Cui, J.; Ning, M.; Jin, P.; and Yuan, L. 2023. Video-llava: Learning united visual representation by alignment before projection. *arXiv preprint arXiv:2311.10122*.

Lin, J.; Tang, J.; Tang, H.; Yang, S.; Chen, W.-M.; Wang, W.-C.; Xiao, G.; Dang, X.; Gan, C.; and Han, S. 2024. Awq: Activation-aware weight quantization for on-device llm compression and acceleration. *Proceedings of machine learning and systems*, 6: 87–100.

Liu, A.; Feng, B.; Xue, B.; Wang, B.; Wu, B.; Lu, C.; Zhao, C.; Deng, C.; Zhang, C.; Ruan, C.; et al. 2024a. Deepseek-v3 technical report. *arXiv preprint arXiv:2412.19437*.

Liu, H.; Li, C.; Li, Y.; and Lee, Y. J. 2024b. Improved baselines with visual instruction tuning. In *Proceedings of the IEEE/CVF conference on computer vision and pattern recognition*, 26296–26306.

Liu, H.; Li, C.; Li, Y.; Li, B.; Zhang, Y.; Shen, S.; and Lee, Y. J. 2024c. Llavanext: Improved reasoning, ocr, and world knowledge.

Liu, H.; Li, C.; Wu, Q.; and Lee, Y. J. 2023. Visual instruction tuning. *Advances in neural information processing systems*, 36: 34892–34916.

Liu, T.; Shi, L.; Hong, R.; Hu, Y.; Yin, Q.; and Zhang, L. 2024d. Multi-stage vision token dropping: Towards efficient multimodal large language model. *arXiv preprint arXiv:2411.10803*.

Liu, X.; Wang, Y.; Ma, J.; and Zhang, L. 2025. Video Compression Commander: Plug-and-Play Inference Acceleration for Video Large Language Models. *arXiv preprint arXiv:2505.14454*.

Liu, Y.; Duan, H.; Zhang, Y.; Li, B.; Zhang, S.; Zhao, W.; Yuan, Y.; Wang, J.; He, C.; Liu, Z.; et al. 2024e. Mmbench: Is your multi-modal model an all-around player? In *European conference on computer vision*, 216–233. Springer.

Liu, Y.; Li, Z.; Huang, M.; Yang, B.; Yu, W.; Li, C.; Yin, X.-C.; Liu, C.-L.; Jin, L.; and Bai, X. 2024f. Ocrbench: on the hidden mystery of ocr in large multimodal models. *Science China Information Sciences*, 67(12): 220102.

Lv, C.; Chen, H.; Guo, J.; Ding, Y.; and Liu, X. 2024. Ptq4sam: Post-training quantization for segment anything. In *Proceedings of the IEEE/CVF Conference on computer vision and pattern recognition*, 15941–15951.

Ma, X.; Fang, G.; and Wang, X. 2023. Llm-pruner: On the structural pruning of large language models. *Advances in neural information processing systems*, 36: 21702–21720.

q8 team. 2026. q8.

Saikh, T.; Ghosal, T.; Mittal, A.; Ekbal, A.; and Bhattacharyya, P. 2022. Scienceqa: A novel resource for question answering on scholarly articles. *International Journal on Digital Libraries*, 23(3): 289–301.

Shang, Y.; Cai, M.; Xu, B.; Lee, Y. J.; and Yan, Y. 2024. Llava-prumerge: Adaptive token reduction for efficient large multimodal models. *arXiv preprint arXiv:2403.15388*.

Shao, K.; Tao, K.; Qin, C.; You, H.; Sui, Y.; and Wang, H. 2025. HoliTom: Holistic Token Merging for Fast Video Large Language Models. *arXiv preprint arXiv:2505.21334*.

Shen, L.; Gong, G.; He, T.; Zhang, Y.; Liu, P.; Zhao, S.; and Ding, G. 2025. Fastvid: Dynamic density pruning for fast video large language models. *arXiv preprint arXiv:2503.11187*.

Shi, Y.; Long, Q.; and Wang, W. 2025. Static or Dynamic: Towards Query-Adaptive Token Selection for Video Question Answering. *arXiv preprint arXiv:2504.21403*.

Singh, A.; Natarajan, V.; Shah, M.; Jiang, Y.; Chen, X.; Batra, D.; Parikh, D.; and Rohrbach, M. 2019. Towards vqa models that can read. In *Proceedings of the IEEE/CVF conference on computer vision and pattern recognition*, 8317–8326.

Song, D.; Wang, W.; Chen, S.; Wang, X.; Guan, M.; and Wang, B. 2024. Less is more: A simple yet effective token reduction method for efficient multi-modal llms. *arXiv preprint arXiv:2409.10994*.

Sun, M.; Liu, Z.; Bair, A.; and Kolter, J. Z. 2023. A simple and effective pruning approach for large language models. *arXiv preprint arXiv:2306.11695*.

Swaminathan, S.; Garg, D.; Kannan, R.; and Andres, F. 2020. Sparse low rank factorization for deep neural network compression. *Neurocomputing*, 398: 185–196.

Tao, K.; Qin, C.; You, H.; Sui, Y.; and Wang, H. 2025. DyCoke: Dynamic Compression of Tokens for Fast Video Large Language Models. In *Proceedings of the Computer Vision and Pattern Recognition Conference*, 18992–19001.

Tian, S.; Chen, H.; Lv, C.; Liu, Y.; Guo, J.; Liu, X.; Li, S.; Yang, H.; and Xie, T. 2024. Qvd: Post-training quantization for video diffusion models. In *Proceedings of the 32nd ACM International Conference on Multimedia*, 10572–10581.

Tito, R.; Karatzas, D.; and Valveny, E. 2023. Hierarchical multimodal transformers for multipage docvqa. *Pattern Recognition*, 144: 109834.

Touvron, H.; Lavril, T.; Izacard, G.; Martinet, X.; Lachaux, M.-A.; Lacroix, T.; Rozière, B.; Goyal, N.; Hambro, E.; Azhar, F.; et al. 2023. Llama: Open and efficient foundation language models. *arXiv preprint arXiv:2302.13971*.

Vasu, P. K. A.; Faghri, F.; Li, C.-L.; Koc, C.; True, N.; Antony, A.; Santhanam, G.; Gabriel, J.; Grasch, P.; Tuzel, O.; et al. 2025. Fastvlm: Efficient vision encoding for vision language models. In *Proceedings of the Computer Vision and Pattern Recognition Conference*, 19769–19780.

Wang, P.; Bai, S.; Tan, S.; Wang, S.; Fan, Z.; Bai, J.; Chen, K.; Liu, X.; Wang, J.; Ge, W.; et al. 2024a. Qwen2-vl: Enhancing vision-language model’s perception of the world at any resolution. *arXiv preprint arXiv:2409.12191*.

Wang, X.; Zheng, Y.; Wan, Z.; and Zhang, M. 2024b. Svd-ilm: Truncation-aware singular value decomposition for large language model compression. *arXiv preprint arXiv:2403.07378*.

Wen, Z.; Gao, Y.; Wang, S.; Zhang, J.; Zhang, Q.; Li, W.; He, C.; and Zhang, L. 2025. Stop looking for important tokens in multimodal language models: Duplication matters more. *arXiv preprint arXiv:2502.11494*.

Wnag, Z.; Guo, J.; Gong, R.; Yong, Y.; Liu, A.; Huang, Y.; Liu, J.; and Liu, X. 2024. PTSBench: A Comprehensive Post-Training Sparsity Benchmark Towards Algorithms and Models. *arXiv:2412.07268*.

Wu, H.; Li, D.; Chen, B.; and Li, J. 2024. Longvideobench: A benchmark for long-context interleaved video-language understanding. *Advances in Neural Information Processing Systems*, 37: 28828–28857.

Xiao, G.; Lin, J.; Seznec, M.; Wu, H.; Demouth, J.; and Han, S. 2023. Smoothquant: Accurate and efficient post-training quantization for large language models. In *International conference on machine learning*, 38087–38099. PMLR.

Xing, L.; Huang, Q.; Dong, X.; Lu, J.; Zhang, P.; Zang, Y.; Cao, Y.; He, C.; Wang, J.; Wu, F.; et al. 2024. Pyramiddrop: Accelerating your large vision-language models via pyramid visual redundancy reduction. *arXiv preprint arXiv:2410.17247*.

Yang, C.; Sui, Y.; Xiao, J.; Huang, L.; Gong, Y.; Li, C.; Yan, J.; Bai, Y.; Sadayappan, P.; Hu, X.; et al. 2025a. Topv: Compatible token pruning with inference time optimization for fast and low-memory multimodal vision language model. In *Proceedings of the Computer Vision and Pattern Recognition Conference*, 19803–19813.

Yang, S.; Chen, Y.; Tian, Z.; Wang, C.; Li, J.; Yu, B.; and Jia, J. 2025b. Visionzip: Longer is better but not necessary in vision language models. In *Proceedings of the Computer Vision and Pattern Recognition Conference*, 19792–19802.

Ye, X.; Gan, Y.; Ge, Y.; Zhang, X.-P.; and Tang, Y. 2025. Atp-llava: Adaptive token pruning for large vision language models. In *Proceedings of the Computer Vision and Pattern Recognition Conference*, 24972–24982.

Zhai, X.; Mustafa, B.; Kolesnikov, A.; and Beyer, L. 2023. Sigmoid loss for language image pre-training. In *Proceedings of the IEEE/CVF international conference on computer vision*, 11975–11986.

Zhang, K.; Li, B.; Zhang, P.; Pu, F.; Cahyono, J. A.; Hu, K.; Liu, S.; Zhang, Y.; Yang, J.; Li, C.; et al. 2024a. Lmms-eval: Reality check on the evaluation of large multimodal models. *arXiv preprint arXiv:2407.12772*.

Zhang, Q.; Cheng, A.; Lu, M.; Zhang, R.; Zhuo, Z.; Cao, J.; Guo, S.; She, Q.; and Zhang, S. 2024b. Beyond text-visual attention: Exploiting visual cues for effective token pruning in vlms. *arXiv preprint arXiv:2412.01818*.

Zhang, Y.; Fan, C.-K.; Ma, J.; Zheng, W.; Huang, T.; Cheng, K.; Gudovskiy, D.; Okuno, T.; Nakata, Y.; Keutzer, K.; et al. 2024c. Sparsevlm: Visual token sparsification for efficient vision-language model inference. *arXiv preprint arXiv:2410.04417*.

Zhang, Y.; Wu, J.; Li, W.; Li, B.; Ma, Z.; Liu, Z.; and Li, C. 2024d. Video instruction tuning with synthetic data. *arXiv preprint arXiv:2410.02713*.

Zhao, J.; Zhang, Z.; Chen, B.; Wang, Z.; Anandkumar, A.; and Tian, Y. 2024. Galore: Memory-efficient llm training by gradient low-rank projection. *arXiv preprint arXiv:2403.03507*.

Zheng, L.; Yin, L.; Xie, Z.; Sun, C. L.; Huang, J.; Yu, C. H.; Cao, S.; Kozyrakis, C.; Stoica, I.; Gonzalez, J. E.; et al. 2024. Sqlang: Efficient execution of structured language model programs. *Advances in neural information processing systems*, 37: 62557–62583.

Zhou, J.; Shu, Y.; Zhao, B.; Wu, B.; Xiao, S.; Yang, X.; Xiong, Y.; Zhang, B.; Huang, T.; and Liu, Z. 2024. Mlvu: A

comprehensive benchmark for multi-task long video understanding. *arXiv e-prints*, arXiv-2406.

Zhu, D.; Chen, J.; Shen, X.; Li, X.; and Elhoseiny, M. 2023. Minigpt-4: Enhancing vision-language understanding with advanced large language models. *arXiv preprint arXiv:2304.10592*.

# Supplementary Material

## A Related Works

### A.1 Efficient Vision-Language Models

Recent Vision-Language Models (VLMs), such as Flamingo (Alayrac et al. 2022), BLIP-2 (Li et al. 2023a), MiniGPT-4 (Zhu et al. 2023), and Qwen-VL (Wang et al. 2024a), typically follow an encoder-projector-decoder architecture, where visual inputs are encoded into tokens, aligned via a projector (*e.g.*, MLP or Q-Former), and decoded by a language model. To improve visual understanding, these models adopt inputs with high spatial and temporal resolution, resulting in a surge of visual tokens and increased computation. To address this, several efficient strategies have been proposed: 1) BLIP-2 (Li et al. 2023a) introduces Q-Former, which reduces the token count via learned queries. 2) Downsampling methods like bilinear interpolation (LLaVA-OneVision (Li et al. 2024a)) and average pooling (LLaVA-Video (Zhang et al. 2024d)) compress token grids. 3) Pixel unshuffle, used in InternVL (Chen et al. 2024c), decreases spatial tokens by rearranging feature maps. Despite these advances, their substantial model size and computational overhead pose significant challenges for deployment in resource-constrained devices, highlighting the urgent need for more efficient strategies.

### A.2 Training-free Compression

Compared with time-intensive and energy-intensive compression methods such as knowledge distillation (Gou et al. 2021), training-free compression offers a more efficient solution for reducing the cost of VLMs. A primary approach is token compression (Chen et al. 2024b; Zhang et al. 2024c; Bolya et al. 2022; Yang et al. 2025b; Shi, Long, and Wang 2025; Alvar et al. 2025; Liu et al. 2024d; Shang et al. 2024; Arif et al. 2025; Song et al. 2024; Xing et al. 2024; Han et al. 2024; Lan et al. 2024; Ye et al. 2025; Vasu et al. 2025; Han et al. 2025; Yang et al. 2025a; Dhouib et al. 2025; Liu et al. 2025; Tao et al. 2025; Fu et al. 2024; Shen et al. 2025; Huang, Zhou, and Han 2024; Shao et al. 2025), which reduces the number of visual tokens to accelerate inference. These schemes either utilize attention-based (Chen et al. 2024b; Xing et al. 2024; Yang et al. 2025b; Liu et al. 2024d) or similarity-based (Bolya et al. 2022; Alvar et al. 2025; Zhang et al. 2024b) metrics to discard or merge less salient tokens. Recently, several methods (Tao et al. 2025; Fu et al. 2024; Shen et al. 2025; Shao et al. 2025; Shi, Long, and Wang 2025) have also been proposed specifically for videos, aiming to reduce temporal redundancy across consecutive frames. Another direction is model compression, including quantization (Xiao et al. 2023; Frantar et al. 2022; Lin et al. 2024; Chen et al. 2024a; Lv et al. 2024; Tian et al. 2024; Huang et al. 2024, 2025b,a), network pruning (Ma, Fang, and Wang 2023; Frantar and Alistarh 2023; Sun et al. 2023; Wnag et al. 2024; Huang et al. 2025c; J. Guo, W. Ouyang,

and D. Xu 2020; Guo et al. 2020; Guo, Ouyang, and Xu 2020; Guo, Liu, and Xu 2021; Guo, Xu, and Ouyang 2023; He et al. 2025) and low-rank factorization (Zhao et al. 2024; Swaminathan et al. 2020). Among them, quantization stands out as a highly effective and promising approach, offering better performance and compression rate. In this work, we study post-training quantization to complement token reduction and address the memory bottleneck of VLMs.

## B Implementation Details

This section outlines the implementation details for each algorithm. By default, token reduction is applied at the output of the Vision Tower unless otherwise stated in Tab. 4, Tab. 6 and Tab. 7.

- MustDrop (Liu et al. 2024d): MustDrop MS (Liu et al. 2024d) applies a  $3 \times 3$  window for spatial merge in Tab. 3 and Tab. 4.
- ToMe (Bolya et al. 2022): ToMe MS distributes the pruning of tokens evenly across all layers in Tab. 3. In Tab. 4, since ToMe can merge at most 50% of tokens within each layer, we merge the first/last two layers down to 192 tokens, and first/last three layers down to 128 tokens.
- VisionZip (Yang et al. 2025b): For the VisionZip PA+MS, we adhere to the Dominant and Contextual numbers reported in the original publication.
- SparseVLM (Zhang et al. 2024c): For the SparseVLM PA+MS, we follow the token number of Relevant Text Token Selection and Token Recycling in its paper.
- FastVID (Shen et al. 2025): For fair comparison, we remove the segmentation for transitions where the similarity falls below a fixed threshold  $\tau$  in Tab. 6.
- HoliTom (Shao et al. 2025): We set T to 0.8 and achieved a retention rate of 68.9%, while setting T to 0.6 resulted in a retention rate of 52.4% in Tab. 6.
- PruneVid (Huang, Zhou, and Han 2024): The threshold for token reduction in Tab. 7 is set to 0.6.
- DyCoke (Tao et al. 2025): The token reduction rate is set to 0.5 in Tab. 7.

## C Detailed Results

We provide detailed results (Tab. 11, Tab. 12, Tab. 13, Tab. 14, Tab. 15, Tab. 16 and Tab. 17) on each dataset as a supplement to the tables (*i.e.*, Tab. 3, Tab. 4 and Tab. 5) in the main paper. Additionally, Tab. 18 reports the measured prefill and decode latencies, as well as the peak memory usage during runtime on . For both FastV (Chen et al. 2024b) and DART (Wen et al. 2025), the token reduction is applied at the 5-th block of the LLM. Two key observations can be drawn from the results: (1) Token reduction primarily reduces the prefill latency, while its impact on decode latency

Method	Type	GQA	MMB	MME	POPE	TextVQA	VizWiz	ScienceQA	OCRBench
<i>Upper Bound, 576 Tokens (100%)</i>									
LLaVA-1.5-7B (Liu et al. 2023)	-	62.0	64.2	67.0	87.0	46.1	54.3	69.5	31.3
<i>Retain 192 Tokens in Average (<math>\downarrow</math> 66.7%)</i>									
VisionZip (Yang et al. 2025b)	PA	59.3	63.5	63.8	86.4	44.8	54.3	68.6	31.3
VisPruner (Zhang et al. 2024b)	PS	59.6	62.5	62.2	87.6	41.7	55.4	68.3	29.2
DivPrune (Alvar et al. 2025)	PS	59.9	62.4	62.6	87.5	43.3	55.7	68.7	30.0
ToMe (Bolya et al. 2022)	MS	59.1	61.3	61.3	87.5	38.1	55.7	68.4	26.8
VisionZip (Yang et al. 2025b)	MS	58.8	61.3	61.2	85.3	35.8	54.6	68.5	26.3
MustDrop (Liu et al. 2024d)	MS	58.4	63.1	62.2	83.3	40.0	55.7	69.0	28.9
VisionZip (Yang et al. 2025b)	PA+MS	59.2	63.8	63.1	86.5	44.6	54.3	68.5	30.6
<i>Retain 128 Tokens in Average (<math>\downarrow</math> 77.8%)</i>									
VisionZip (Yang et al. 2025b)	PA	57.9	62.5	62.8	84.4	44.3	54.5	68.6	29.9
VisPruner (Zhang et al. 2024b)	PS	58.3	60.9	59.1	86.9	39.6	56.1	68.3	27.8
DivPrune (Alvar et al. 2025)	PS	59.4	62.2	61.3	87.4	41.9	56.1	68.8	28.6
ToMe (Bolya et al. 2022)	MS	58.4	60.6	60.0	87.2	36.0	56.7	68.3	24.6
VisionZip (Yang et al. 2025b)	MS	58.0	59.0	59.0	84.2	31.0	55.6	68.9	25.1
MustDrop (Liu et al. 2024d)	MS	56.8	60.7	57.7	81.5	34.3	56.6	67.8	27.2
VisionZip (Yang et al. 2025b)	PA+MS	57.6	62.2	63.3	84.7	44.2	54.8	68.7	29.9
<i>Retain 64 Tokens in Average (<math>\downarrow</math> 88.9%)</i>									
VisionZip (Yang et al. 2025b)	PA	54.9	60.8	59.5	80.5	42.8	55.9	69.0	28.8
VisPruner (Zhang et al. 2024b)	PS	56.3	58.2	57.9	85.9	35.6	56.7	67.3	24.4
DivPrune (Alvar et al. 2025)	PS	57.8	59.1	57.8	86.3	39.4	57.6	68.2	28.3
ToMe (Bolya et al. 2022)	MS	56.6	58.8	57.5	85.2	31.1	57.3	67.7	21.0
VisionZip (Yang et al. 2025b)	MS	55.9	53.5	55.0	81.7	24.1	57.3	66.6	21.3
MustDrop (Liu et al. 2024d)	MS	53.3	47.1	49.2	77.9	16.5	56.4	64.1	17.8
VisionZip (Yang et al. 2025b)	PA+MS	55.2	60.0	60.4	80.9	42.2	55.5	68.8	28.4

Table 11: Detailed performance of different token reduction methods in Vision Tower (LLaVA-1.5-7B).

Method	Type	GQA	MMB	MME	POPE	TextVQA	VizWiz	ScienceQA	OCRBench
<i>Upper Bound, <math>\sim</math>2880 Tokens (100%)</i>									
LLaVA-NeXT-7B (Liu et al. 2024b)	-	64.3	67.1	66.0	87.6	64.7	60.7	70.1	52.1
<i>Retain <math>\sim</math>640 Tokens in Average (<math>\downarrow</math> 77.8%)</i>									
VisionZip (Yang et al. 2025b)	PA	61.9	65.4	63.0	87.6	61.9	59.9	67.8	48.8
VisPruner (Zhang et al. 2024b)	PS	61.9	63.0	62.2	88.2	53.6	57.9	67.6	36.0
DivPrune (Alvar et al. 2025)	PS	61.4	64.7	65.0	87.2	54.4	58.8	67.5	37.6
VisionZip (Yang et al. 2025b)	MS	61.8	63.6	63.4	84.9	41.1	57.1	67.2	27.7
MustDrop (Liu et al. 2024d)	MS	62.7	65.6	62.9	85.5	49.8	58.2	69.4	32.9
<i>Retain <math>\sim</math>320 Tokens in Average (<math>\downarrow</math> 88.9%)</i>									
VisionZip (Yang et al. 2025b)	PA	59.2	65.4	61.8	85.0	58.6	57.3	67.3	41.6
VisPruner (Zhang et al. 2024b)	PS	59.2	63.0	58.9	86.9	47.7	55.4	68.2	28.1
DivPrune (Alvar et al. 2025)	PS	59.9	64.7	62.1	85.6	49.4	57.5	67.7	33.0
VisionZip (Yang et al. 2025b)	MS	58.9	63.6	58.1	82.9	34.3	55.6	67.7	23.0
MustDrop (Liu et al. 2024d)	MS	61.4	65.6	59.0	82.8	36.3	56.1	67.7	24.8
<i>Retain <math>\sim</math>160 Tokens in Average (<math>\downarrow</math> 94.4%)</i>									
VisionZip (Yang et al. 2025b)	PA	54.9	65.4	56.5	81.0	54.3	55.8	67.7	33.1
VisPruner (Zhang et al. 2024b)	PS	55.5	63.0	53.1	82.7	41.9	54.2	66.9	21.9
DivPrune (Alvar et al. 2025)	PS	58.0	64.7	59.5	83.1	45.1	57.6	68.1	26.6
VisionZip (Yang et al. 2025b)	MS	55.8	63.6	50.0	77.8	25.0	54.3	66.4	15.4

Table 12: Detailed performance of different token reduction methods in Vision Tower (LLaVA-NeXT-7B).

Method	Type	GQA	MMB	MME	POPE	TextVQA	VizWiz	ScienceQA	OCRBench
<i>Upper Bound, 100% Tokens</i>									
Qwen2.5-VL-7B	-	60.4	82.9	83.3	87.4	82.9	70.8	87.4	83.7
<i>Retain 33.3% Tokens in Average (<math>\downarrow</math> 66.7%)</i>									
VisionZip (Yang et al. 2025b)	PA	58.9	82.8	81.9	86.7	78.7	69.4	86.7	73.4
VisPruner (Zhang et al. 2024b)	PS	58.6	80.7	81.2	86.2	76.4	69.2	85.3	69.2
DivPrune (Alvar et al. 2025)	PS	59.6	81.4	80.0	86.6	78.9	69.6	84.9	72.9
VisionZip (Yang et al. 2025b)	MS	59.5	80.8	80.1	86.1	74.7	70.9	86.0	70.3
<i>Retain 22.2% Tokens in Average (<math>\downarrow</math> 77.8%)</i>									
VisionZip (Yang et al. 2025b)	PA	57.1	80.5	79.3	85.9	74.6	68.6	85.4	63.5
VisPruner (Zhang et al. 2024b)	PS	57.3	79.1	77.6	84.6	70.2	67.9	84.4	58.1
DivPrune (Alvar et al. 2025)	PS	58.7	78.9	77.7	85.6	75.1	69.1	84.3	65.8
VisionZip (Yang et al. 2025b)	MS	58.4	79.6	79.5	85.4	66.0	69.5	83.8	59.8
<i>Retain 11.1% Tokens in Average (<math>\downarrow</math> 88.9%)</i>									
VisionZip (Yang et al. 2025b)	PA	52.6	76.9	70.0	82.9	62.9	67.1	82.9	42.8
VisPruner (Zhang et al. 2024b)	PS	54.0	73.8	71.4	81.1	54.9	64.6	81.8	40.9
DivPrune (Alvar et al. 2025)	PS	56.2	75.7	72.4	82.4	65.5	66.4	82.1	50.1
VisionZip (Yang et al. 2025b)	MS	55.9	74.5	73.5	82.5	45.2	66.5	80.0	43.7

Table 13: Detailed performance of different token reduction methods in Vision Tower (Qwen2.5-VL-7B).

Method	Type	GQA	MMB	MME	POPE	TextVQA	VizWiz	ScienceQA	Prefill
<i>Upper Bound, 576 Tokens (100%)</i>									
LLaVA-1.5-7B (Liu et al. 2023)	-	62.0	64.2	67.0	87.0	46.1	54.3	69.5	27.3 ms
<i>Retain 192 Tokens in Average (<math>\downarrow</math> 66.7%)</i>									
ToMe* (Bolya et al. 2022)	MS	53.1	52.0	56.3	77.3	15.5	54.5	65.8	16.6 ms
ToMe† (Bolya et al. 2022)	MS	59.4	63.2	62.3	87.0	38.7	56.6	69.5	16.6 ms
MustDrop* (Liu et al. 2024d)	MS	56.9	60.2	56.9	83.9	30.8	54.9	67.7	16.6 ms
MustDrop† (Liu et al. 2024d)	MS	58.4	63.1	62.2	83.3	40.0	55.7	69.0	16.6 ms
<i>Retain 128 Tokens in Average (<math>\downarrow</math> 77.8%)</i>									
ToMe* (Bolya et al. 2022)	MS	44.2	36.2	44.6	64.4	10.4	53.6	63.9	15.8 ms
ToMe† (Bolya et al. 2022)	MS	57.7	61.1	60.9	84.7	32.1	56.6	69.0	16.0 ms
MustDrop* (Liu et al. 2024d)	MS	52.6	52.8	53.2	78.0	22.7	54.5	65.6	16.0 ms
MustDrop† (Liu et al. 2024d)	MS	56.8	60.7	57.7	81.5	34.3	56.6	67.8	16.2 ms

Table 14: Detailed results of token reduction at different layers in Vision Tower (LLaVA-1.5-7B). \* and † denote merging in the first and last layer.

and peak memory is negligible. (2) As the model size increases, *e.g.*, from LLaVA-1.5-7B to LLaVA-1.5-13B, the acceleration effect on the prefill stage becomes more pronounced when maintaining the same proportion of retained visual tokens ( $\sim 2.0 \times$  vs.  $\sim 1.5 \times$ ).

## D Visualization

### D.1 Visualization Examples

In Fig. 4, we present qualitative results of different algorithms on the GQA (Hudson and Manning 2019) dataset. We observe that text-guided strategies, particularly FastV (Chen et al. 2024b) and SparseVLM (Zhang et al. 2024c), tend to retain a significant amount of irrelevant background. For example, the black background near the text region, which is

located at the bottom of the image, is often preserved. This also explains why DART (Wen et al. 2025) achieves better accuracy compared to the other two algorithms, as it retains only a very small number of pivot text-relevant tokens and therefore preserves relatively less background information. Therefore, in LLMs, relying entirely on the question prompt to guide token pruning can lead to unsatisfactory results.

In comparison, pruning methods (Yang et al. 2025b; Alvar et al. 2025) in Vision Tower lack access to textual information, which leads to reduced attention to the question prompt. This can be observed in the second image, where objects such as “table” or “couch” receive less focus.

Method	Type	GQA	MMB	MME	POPE	TextVQA	VizWiz	ScienceQA	OCRBench
<i>Upper Bound, 576 Tokens (100%)</i>									
LLaVA-1.5-7B (Liu et al. 2023)	-	62.0	64.2	67.0	87.0	46.1	54.3	69.5	31.3
<i>Retain 192 Tokens in Average (<math>\downarrow</math> 66.7%)</i>									
FastV (Chen et al. 2024b)	PA	58.4	63.5	64.5	83.7	43.5	54.4	69.2	28.5
SparseVLM (Zhang et al. 2024c)	PA	60.2	63.4	66.4	85.6	44.4	54.2	69.2	30.5
DART (Wen et al. 2025)	PS	60.8	64.4	66.6	85.0	44.8	54.6	69.4	30.0
HoliTom (Shao et al. 2025)	MS	59.2	58.8	63.5	84.4	42.7	55.8	65.8	29.0
SparseVLM (Zhang et al. 2024c)	PA+MS	59.9	63.2	66.5	85.7	44.4	54.2	68.9	30.0
<i>Retain 128 Tokens in Average (<math>\downarrow</math> 77.8%)</i>									
FastV (Chen et al. 2024b)	PA	56.1	62.1	63.0	81.0	39.6	54.3	70.2	26.2
SparseVLM (Zhang et al. 2024c)	PA	58.6	63.1	65.1	84.1	42.2	54.6	69.4	28.3
DART (Wen et al. 2025)	PS	59.5	63.8	65.4	83.9	43.5	54.7	69.7	29.8
HoliTom (Shao et al. 2025)	MS	57.8	57.0	62.0	82.8	39.2	55.4	66.4	26.6
SparseVLM (Zhang et al. 2024c)	PA+MS	58.6	63.2	65.1	84.7	42.5	54.3	69.6	27.9
<i>Retain 64 Tokens in Average (<math>\downarrow</math> 88.9%)</i>									
FastV (Chen et al. 2024b)	PA	52.2	58.3	57.8	75.1	32.1	53.4	68.6	18.8
SparseVLM (Zhang et al. 2024c)	PA	55.9	62.8	61.3	79.9	36.9	53.3	69.7	23.0
DART (Wen et al. 2025)	PS	56.8	61.6	64.9	80.7	41.2	54.7	69.9	27.0
HoliTom (Shao et al. 2025)	MS	55.6	55.5	59.5	79.0	31.7	54.9	66.2	21.6
SparseVLM (Zhang et al. 2024c)	PA+MS	56.0	62.3	61.9	83.0	37.9	53.2	69.6	24.3

Table 15: Detailed performance of different token reduction methods in LLM (LLaVA-1.5-7B).

Method	Type	GQA	MMB	MME	POPE	TextVQA	VizWiz	ScienceQA	OCRBench
<i>Upper Bound, <math>\sim</math>2880 Tokens (100%)</i>									
LLaVA-NeXT-7B (Liu et al. 2024b)	-	64.3	67.1	66.0	87.6	64.7	60.7	70.1	52.1
<i>Retain <math>\sim</math>640 Tokens in Average (<math>\downarrow</math> 77.8%)</i>									
FastV (Chen et al. 2024b)	PA	61.0	64.8	63.0	86.1	58.6	59.0	68.2	38.9
SparseVLM (Zhang et al. 2024c)	PA	62.3	65.8	63.8	86.7	60.8	60.3	68.6	42.0
DART (Wen et al. 2025)	PS	63.0	65.4	64.2	86.5	62.2	60.6	68.8	44.2
HoliTom (Shao et al. 2025)	MS	61.6	62.2	61.0	86.6	57.0	58.7	65.8	34.0
<i>Retain <math>\sim</math>320 Tokens in Average (<math>\downarrow</math> 88.9%)</i>									
FastV (Chen et al. 2024b)	PA	56.1	63.2	56.6	81.9	49.4	56.9	67.7	24.8
SparseVLM (Zhang et al. 2024c)	PA	59.7	64.8	62.7	85.0	53.8	59.1	68.9	30.4
DART (Wen et al. 2025)	PS	60.7	63.9	62.5	84.2	58.2	59.4	67.9	35.4
HoliTom (Shao et al. 2025)	MS	58.3	59.4	58.5	83.4	48.9	56.1	65.9	24.8
<i>Retain <math>\sim</math>160 Tokens in Average (<math>\downarrow</math> 94.4%)</i>									
FastV (Chen et al. 2024b)	PA	51.0	56.1	50.9	74.2	38.5	55.1	65.9	15.4
SparseVLM (Zhang et al. 2024c)	PA	56.2	63.1	58.5	80.9	45.6	56.9	67.7	19.8
DART (Wen et al. 2025)	PS	57.1	61.5	58.8	79.6	52.0	57.9	68.1	26.8
HoliTom (Shao et al. 2025)	MS	38.4	54.4	51.3	79.4	38.4	54.4	65.9	16.9

Table 16: Detailed performance of different token reduction methods in LLM (LLaVA-NeXT-7B).

## D.2 Similarity in Video

We utilize cosine similarity to analyze the redundancy between visual tokens. As shown in Fig. 5, LLaVA-OneVision(Li et al. 2024a) encodes the video into 32 frames, each represented by 196 feature tokens. We group the tokens from four frames into a single subplot, resulting in a total of eight subplots. To enhance clarity, we visualize only the top 10% of token similarities. Two types of redundancy

mentioned in the main paper (*i.e.*, spatial and temporal redundancy), can be clearly observed from the figure.

For spatial redundancy, we observe from the cosine similarities in frames 16-19 (*i.e.*, subplot 5) that each frame contains a high degree of intra-frame similarity. In addition, temporal redundancy is primarily reflected in the same spatial positions across different frames, specifically between token indices at positions  $idx$  and  $idx + 196n$ , where  $n$  is an integer.

Method	Type	GQA	MMB	MME	POPE	TextVQA	VizWiz	ScienceQA	OCRBench
<i>Upper Bound, 100% Tokens</i>									
Qwen2.5-VL-7B	-	60.4	82.9	83.3	87.4	82.9	70.8	87.4	83.7
<i>Retain 33.3% Tokens in Average (<math>\downarrow</math> 66.7%)</i>									
FastV (Chen et al. 2024b)	PA	55.0	79.6	78.9	84.2	78.9	69.1	85.8	61.2
SparseVLM (Zhang et al. 2024c)	PA	57.0	82.0	80.9	86.9	80.9	69.8	86.0	63.8
DART (Wen et al. 2025)	PS	58.4	80.9	80.6	84.9	77.5	68.9	85.0	65.7
Holitom (Shao et al. 2025)	MS	58.0	81.4	78.5	85.8	79.6	69.8	87.4	62.9
<i>Retain 22.2% Tokens in Average (<math>\downarrow</math> 77.8%)</i>									
FastV (Chen et al. 2024b)	PA	51.4	75.3	74.4	81.6	75.1	67.3	82.2	49.1
SparseVLM (Zhang et al. 2024c)	PA	55.1	80.4	80.2	85.1	78.6	68.8	84.3	53.3
DART (Wen et al. 2025)	PS	56.5	79.7	78.5	82.5	72.3	68.6	84.0	55.6
Holitom (Shao et al. 2025)	MS	56.7	78.2	76.5	84.8	76.3	68.0	84.7	55.3
<i>Retain 11.1% Tokens in Average (<math>\downarrow</math> 88.9%)</i>									
FastV (Chen et al. 2024b)	PA	45.3	62.9	65.4	72.4	63.5	63.0	78.8	30.3
SparseVLM (Zhang et al. 2024c)	PA	51.5	74.1	76.2	81.6	71.2	66.8	82.4	31.4
DART (Wen et al. 2025)	PS	52.2	73.7	73.4	77.5	61.1	65.3	81.5	43.6
Holitom (Shao et al. 2025)	MS	53.5	73.1	70.3	79.4	66.5	64.3	81.7	38.6

Table 17: Detailed performance of different token reduction methods in LLM (Qwen2.5-VL-7B).

Model	Token Number	Prefill (ms)	Decode (ms)	Peak Memory (GB)
LLaVA-1.5-7B (Liu et al. 2023)	576	27.2	18.1	13.9
ToMe (Bolya et al. 2022)	128	17.7	17.6	13.4
VisionZip (Yang et al. 2025b)	128	17.5	17.4	13.5
DivPrune (Alvar et al. 2025)	128	17.3	17.6	13.4
FastV (Chen et al. 2024b)	128	19.1	17.7	13.5
DART (Wen et al. 2025)	128	22.9	17.7	13.5
LLaVA-1.5-13B (Liu et al. 2023)	576	44.6	17.9	26.1
ToMe (Bolya et al. 2022)	128	22.6	17.6	25.4
VisionZip (Yang et al. 2025b)	128	23.0	17.6	25.4
DivPrune (Alvar et al. 2025)	128	21.5	17.6	25.3
FastV (Chen et al. 2024b)	128	25.8	17.6	25.5
DART (Wen et al. 2025)	128	27.4	17.5	25.4

Table 18: The actual latency and memory usage profiles of different algorithms.

### D.3 Multi-Turn Dialogue Task

Fig. 6 shows the visualization of multi-turn dialogues. Specifically, we perform visual token pruning using each algorithm in the first turn and examine their responses to the question in the second turn. It is worth noting that if Question 2 is asked in the first turn, all five algorithms generate the same response: “Yes, there is a frisbee to the left of the person in the middle.” However, when the same question is asked in the second turn, the two text-relevant methods (*i.e.*, FastV and SparseVLM) produce unsatisfactory responses. This further demonstrates that these text-guided token reduction methods are highly dependent on the current-turn question, which may affect the model’s ability to answer questions in subsequent turns.

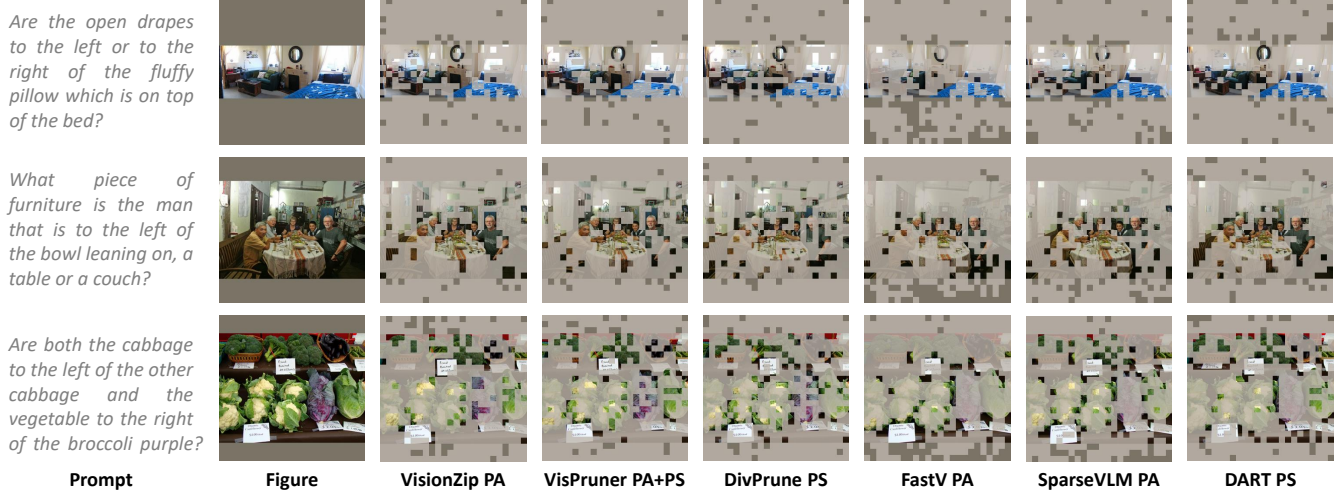


Figure 4: Qualitative results of GQA (Hudson and Manning 2019) benchmark on LLaVA-1.5-7B (Liu et al. 2023).

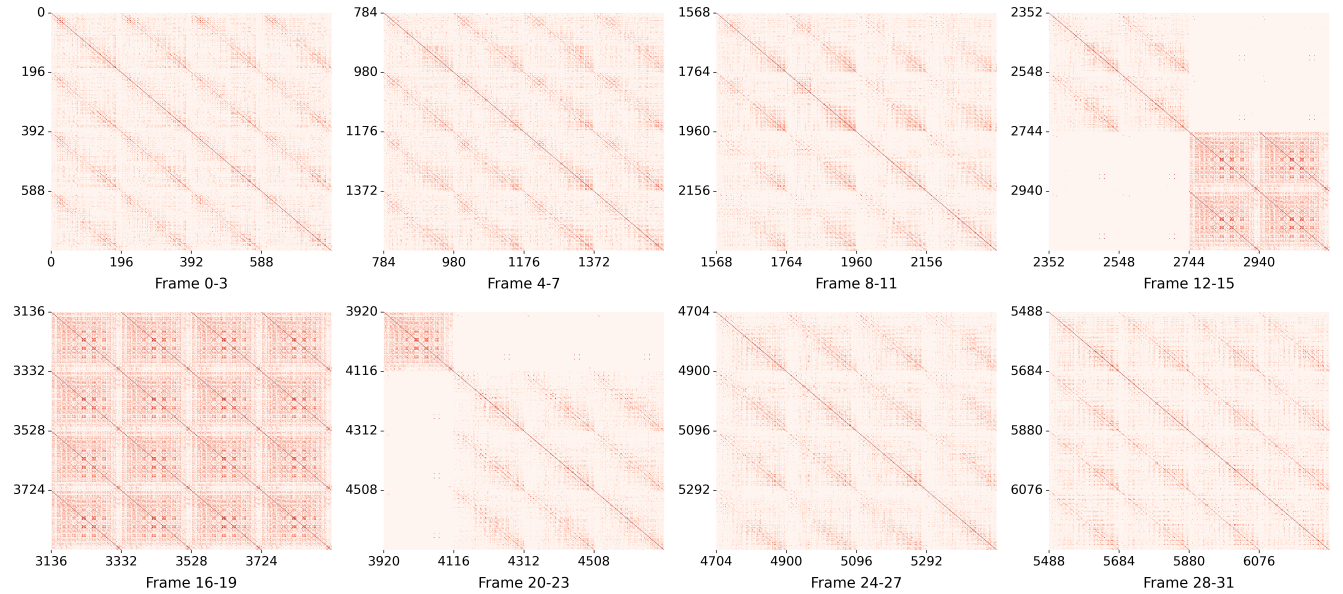


Figure 5: Visual Token similarities in LLaVA-OneVision (Li et al. 2024a).



-  **Question1:** Is the shirt the same color as the building?
-  **Question2:** Is there a frisbee to the left of the person in the middle?
-  **VisionZip:** Yes, there is a frisbee to the left of the person in the middle.
-  **DivPrune:** Yes, there is a frisbee to the left of the person in the middle.
-  **DART:** Yes, there is a frisbee to the left of the person in the middle.
-  **FastV:** No, there is no frisbee to the left of the person in the middle.  
The frisbee is to the right of the person in the middle.
-  **SparseVLM:** No, there is no frisbee to the left of the person in the middle.  
The frisbee is to the right of the person in the middle.

Figure 6: Visualization of multi-turn dialogues across different algorithms.